The Island Arc (2005) **14,** 55–68

Research Article

Late Paleozoic adakites and Nb-enriched basalts from northern Xinjiang, northwest China: Evidence for the southward subduction of the Paleo-Asian Oceanic Plate

HAIXIANG ZHANG,[1,2,*] HECAI NIU,[1] HIROAKI SATO,[2] XUEYUAN YU,[1] QIANG SHAN,[1] BOYOU ZHANG,[1] JUN'ICHI ITO[2] AND TAKASHI NAGAO[3]

[1]*Guangzhou Institute of Geochemistry, Chinese Academy of Sciences, Guangzhou 510640, China (email: zhanghx@gig.ac.cn),* [2]*Department of Earth and Planetary Sciences, Faculty of Science, Kobe University, Kobe 657-8501, Japan and* [3]*Center for Instrumental Analyses, Yamaguchi University, Yoshida 1677-1, Yamaguchi 753-8512, Japan*

Abstract Volcanic rocks consisting of adakite and Nb-enriched basalt are found in the early Devonian Tuoranggekuduke Group in the northern margin of the Kazakhstan-Junggar Plate, northern Xinjiang, northwest China. The geochemical characteristics of the andesitic and dacitic rocks in this area resemble that of adakites. The relatively high Al_2O_3, Na_2O and MgO content and $Mg^{\#}$ values indicate that the adakites were generated in relation to oceanic slab subduction rather than the partial melting of basaltic crust. A slightly higher SrI and a lower $\varepsilon_{Nd}(t = 375\ Ma)$ compared to adakites of mid-oceanic ridge basalt (MORB) imply that slab sediments were incorporated into these adakites during slab melting. The Nb-enriched basalt lavas, which are intercalated in adakite lava suite, are silica saturated and are distinguished from the typical arc basalts by their higher Nb and Ti content (high field strength element enrichment). They are derived from the partial melting of the slab melt-metasomatized mantle wedge peridotite. Apparently, positive Sr anomalies and a slightly higher heavy rare earth element content in these adakites compared to their Cenozoic counterparts indicate that the geothermal gradient in the Paleo-Asian Oceanic subduction zone and the depth of the Paleo-Asian Oceanic slab melting are between those of their Archean and Cenozoic counterparts. The distribution of the adakites and Nb-enriched basalts in the northern margin of the Kazakhstan-Junggar Plate, northern Xinjiang, indicates that the Paleo-Asian Oceanic Plate subducted southward beneath the Kazakhstan-Junggar Plate in the early Devonian period.

Key words: adakite, Central Asian Orogenic Belt, Kazakhstan-Junggar Plate, Nb-enriched basalt, Paleo-Asian Ocean, subduction.

INTRODUCTION

The association between adakite and Nb-enriched basalt has a geotectonic significance because of its close relationship with the subduction of young oceanic slab. Most adakites and Nb-enriched basalts were distributed in the arcs around the Pacific Ocean in the Cenozoic era, such as Mount St Helens of the Cascade volcanic chain (Defant *et al.* 1992; Defant & Drummond 1993); western Panama and southeastern Costa Rica (Defant *et al.* 1992); Kamchatka, Russia (Kepezhinskas *et al.* 1996); west Mindanao, Philippines (Sajona *et al.* 1993; 1994; 1996; 2000); Vizcaino Peninsula, Mexico (Robles *et al.* 2001); and southwest Japan (Morris 1995; Kimura *et al.* 2002; 2003; Tamura *et al.* 2003). A few of them are found in Archean greenstone belts, such as Wawa, Birch-

*Correspondence.

Received 28 January 2004; accepted for publication 4 November 2004.

Uchi and Pickle Lake of Superior Province, Canada (Hollings & Kerrich 2000; Polat & Kerrich 2001; Hollings 2002) and usually regarded as evidence of the melting of subducted oceanic slab. The authors have found similar mixtures of adakite and Nb-enriched basalt in the Devonian strata in the northern margin of the Kazakhstan-Junggar Plate, northern Xinjiang, northwest China. These might be related to the southward subduction of the Paleo-Asian Oceanic slab. The aim of this paper is to document the geochemical features of the adakites and Nb-enriched basalts. The origin of these magmas is best explained by the melting of a southward subducted Paleo-Asian Oceanic slab beneath the Kazakhstan-Junggar plate, and this is discussed in detail later.

GEOLOGY, SAMPLES AND ANALYTICAL METHODS

The northern Xinjiang area tectonically belongs to the Central Asian Orogenic Belt (CAOB) that is located between the Siberian and Sino–Korean–Tarim cratons (Fig. 1a). CAOB is immense in size and its geology is poorly understood in the areas outside of the former USSR and China. Sengör *et al.* (1993) suggested that the CAOB, nearly half of which was derived from the mantle by arc accretion, consists mainly of materials commonly found in present-day subduction–accretion complexes, intruded by vast plutons of mainly magmatic arc in origin and covered in places by their derivatives. Project IGCP-420 was established in 1997 and ran for 5 years to investigate the tectonic and struc-

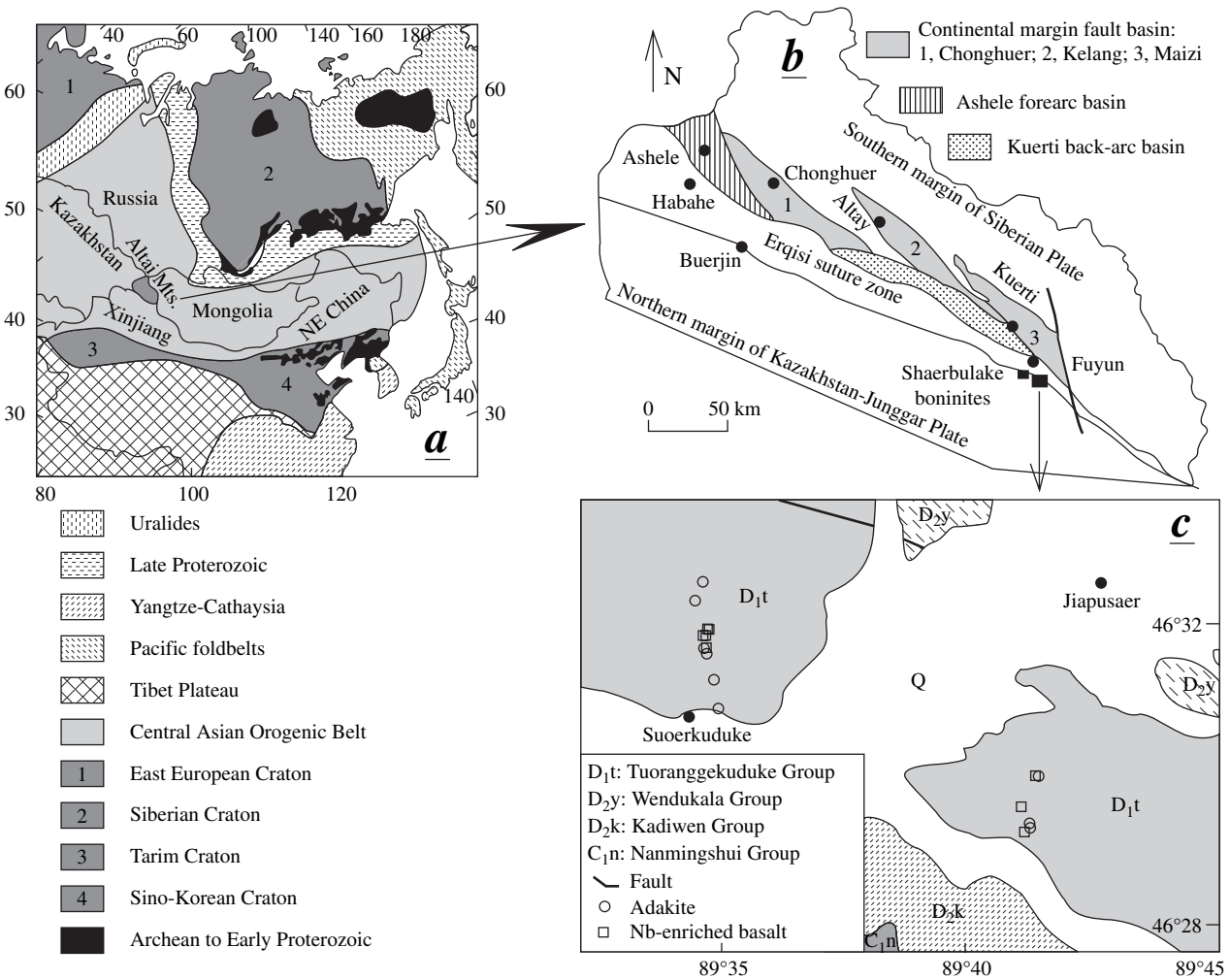

Fig. 1 (a) Simplified tectonic divisions in Asia (reproduced from Jahn *et al.* 2000, with permission). The Central Asian Orogenic Belt (CAOB) includes a vast region of Kazakhstan, western Russia, northwestern China, Mongolia and northeastern China. The study area (northern Xinjiang) is located in the middle of the CAOB. (b) Geotectonic sketch of northern Xinjiang (reproduced from Yu *et al.* 1995, with permission). The Erqisi Suture Zone between the Siberian Plate and the Kazakhstan-Junggar Plate is considered to be the suture belt of the Paleo-Asian Ocean. In the southern margin of the Siberian Plate, the Ashele forearc basin and the Kuerti back-arc basin have been identified from the high-Mg andesites and back-arc basin ophiolites, respectively. (c) Geological map of the study area and sample locations. Adakites and Nb-enriched basalts are interbedded and distributed in the early Devonian Tuoranggekuduke Group.

tural evolution of the orogenic belts and the growth history of the continent crust in the Phanerozoic era. The project showed that the CAOB appears to have been formed by the assembly of Precambrian continental slivers, some of which could be microcontinental fragments, and a lot more of which are Phanerozoic juvenile crust produced by both lateral accretion of arc complexes and vertical under-plating of magmatic materials of mantle origin. Arc accretion appears to have been the dominant process in the formation of the CAOB and complicated subduction–accretion and collision processes may have taken place continuously throughout the Phanerozoic era in Central Asia (Jahn & Capdevila 2000; Jahn *et al.* 2004). Recent studies indicate that most of the Phanerozoic granitoids of the CAOB are characterized by low initial Sr isotopic ratios, positive $\varepsilon_{Nd}(t)$ (ε_{Nd} value at the time of formation) values and young Sm–Nd model ages relative to depleted mantle (T_{DM}) of 300–1200 Ma, which is very different from the coeval granitoids emplaced in some 'classic' orogenic belts, such as the European Caledonides, and the Hercynides and Cathaysia of southeast China and South Korea (Jahn *et al.* 2000; Chen & Jahn 2004). These depleted isotopic compositions suggest a high proportion of the mantle component in their petrogeneses. The massive juvenile continental crust was generated in Central Asia during the Phanerozoic era.

The Altai Mountains straddle four countries: Russia, Kazakhstan, China and Mongolia, and are composed of continental slivers surrounded by island arc accretionary prisms and ophiolite complexes. North Xinjiang is situated in the south Altai Mountains (Fig. 1a). Previous studies suggested that northern Xinjiang comprises a complex mosaic of continental fragments, island arcs and ocean basins with an age between 1000 and 570 Ma (Coleman 1989; Kepezhinskas *et al.* 1991; Amelin *et al.* 1996; 1997; Hu *et al.* 2000; Khain *et al.* 2002). The occurrence of the Paleozoic Paleo-Asian Ocean in northern Xinjiang was defined by the ages of the ophiolites found in this area. The Erqisi Suture Zone between the Siberian Plate and the Kazakhstan-Junggar Plate was thought to be the suture belt of the Paleo-Asian Ocean (He *et al.* 1990; Xiao *et al.* 1992). High-Mg andesites and Mg-rich dacites were found in the Ashele Group in the southern margin of the Siberian Plate (Niu *et al.* 1999), while the fossils found in the sedimentary rocks among the volcanic rock layers in the Ashele Group have been dated as Early to Middle Devonian (Xiao *et al.* 1992). This means that this area was an ancient arc or forearc environment during the Devonian era (Niu *et al.* 1999; Fig. 1b). On the southeast side of the Ashele Arc volcanic rocks, a back-arc basin ophiolite—the Kuerti ophiolite that was produced by subduction of the Paleo-Asian Oceanic slab—has been identified (Xu *et al.* 2003; Fig. 1b). Geological and geotectonic studies on the southern margin of the Siberian Plate led previous researchers to conclude that the Paleo-Asian Oceanic slab subducted northward beneath the Siberian Plate in the Middle to Early Devonian era because arc–back-arc materials were accreted to the Siberian Plate from the south (Xiao *et al.* 1992; Niu *et al.* 1999; Xu *et al.* 2003) (Fig. 1b). This paper discusses the southward subduction of the Paleo-Asian Oceanic slab beneath the Kazakhstan-Junggar Plate as evidenced by the adakite and Nb-enriched basalt combination that occurred in the northern margin of the Kazakhstan-Junggar Plate where the late Paleozoic volcanic rocks are widely distributed. The adakite and Nb-enriched basalt combination belongs to the early Devonian Tuoranggekuduke Group that consists of four parts. From the bottom to the top, they can be described as follows: (i) basalt lava, volcanic tuff breccia, volcanic agglomerate, ferruginous silicalite; (ii) tuff, andesite and dacite lavas; (iii) crystal tuff, tuff breccia, basalt lava; and (iv) tuff, basalt lava, andesite and dacite lavas. The samples in this study were collected from an area near Suoerkuduke in Fuyun County (Fig. 1c).

The analysis of major elements was carried out using the X-ray fluorescence (XRF) spectrometer at the Center for Instrumental Analyses, Yamaguchi University, Japan, or a Varian Vista PRO inductively coupled plasma–atomic emission spectroscopy (ICP–AES) at the Guangzhou Institute of Geochemistry, Chinese Academy of Sciences. The procedures for the analysis of major elements using the XRF and ICP–AES were similar to those described by Nagao *et al.* (1997) and Ramsey *et al.* (1995), respectively. The precision and accuracy of the XRF and ICP–AES in analyzing the major elements are generally better than 5% (Table 1). Trace elements and Nd and Sr isotopes were analyzed at the Guangzhou Institute of Geochemistry, Chinese Academy of Sciences. The procedure for the trace element analysis using a Perkin-Elmer Sciex ELAN 6000 inductively coupled plasma–mass spectrometry (ICP–MS) was similar to that described by Li (1997) and the precision and accuracy of the ICP–MS in analyzing the trace elements are better than 5% (Table 2).

Table 1 Major element compositions of the samples (wt%)[†]

Sample	Adakites							Nb-enriched basalts								
	A01-2	A03-2	A06-3	A10-2	FY-30	FY-53	FY-63	FY-01	FY-12	A04-1	A05-1	FY-16	FY-20	FY-25	FY-26	FY-52	FY-58	FY-59
SiO_2	56.04	57.26	56.47	58.19	54.47	59.90	58.50	64.21	64.52	51.23	51.22	54.21	50.33	51.13	49.86	54.09	52.96	53.82
TiO_2	0.77	1.02	0.80	0.68	0.91	0.71	0.83	0.61	0.61	3.05	3.07	1.85	2.17	3.21	3.66	2.09	2.09	2.31
Al_2O_3	18.54	15.49	16.56	17.78	18.06	18.41	18.86	17.02	17.20	14.20	14.02	16.23	16.84	14.94	15.88	16.13	16.22	15.96
Fe_2O_3	8.64	11.27	9.41	7.92	8.82	6.30	7.07	5.38	5.35	12.63	12.72	10.31	11.73	13.11	13.08	10.31	11.26	11.31
MnO	0.14	0.16	0.16	0.12	0.17	0.10	0.11	0.07	0.07	0.23	0.23	0.18	0.19	0.22	0.18	0.16	0.19	0.19
MgO	3.96	5.08	5.08	3.09	5.08	3.11	3.56	1.74	1.84	4.20	4.39	4.45	5.62	3.98	4.25	4.08	4.89	4.21
CaO	5.09	4.21	4.80	6.40	6.47	4.95	5.64	4.52	4.56	7.09	6.93	5.44	6.56	7.16	6.98	6.72	7.39	7.83
Na_2O	4.92	4.04	5.33	4.50	4.59	5.11	4.30	5.12	4.50	3.42	3.42	3.07	4.25	3.94	4.17	3.86	3.12	1.68
K_2O	1.67	1.31	1.12	1.09	1.13	1.14	0.86	1.12	1.13	2.36	2.41	3.55	1.57	0.79	0.80	1.80	1.01	1.78
P_2O_5	0.23	0.16	0.26	0.23	0.30	0.27	0.27	0.21	0.22	1.58	1.59	0.71	0.73	1.52	1.14	0.76	0.87	0.90
$Mg^{\#}$	47.8	47.4	51.9	43.8	53.5	49.7	50.2	39.3	40.7	40.0	40.8	46.4	48.9	37.8	39.4	44.2	46.5	42.7

[†]A01-2, A03-2, A06-3, A10-2, A04-1 and A05-1 were analyzed by inductively coupled plasma–atomic emission spectroscopy (ICP–AES), whereas the rest were analyzed by X-ray fluorescence (XRF). All data have been recalculated to 100% loss on ignition (LOI)-free.

Nd and Sr isotopes were analyzed by a Micromass Isoprobe multichannel inductively coupled plasma mass spectrometry (MC-ICPMS) spectrometer (Liang *et al.* 2003), with $^{143}Nd/^{144}Nd = 0.511996 \pm 8$ for the Shin Etsu JNdi-1 standard and $^{87}Sr/^{86}Sr = 0.710282 \pm 15$ for NBS987 of the National Bureau of Standards (Table 3).

PETROGRAPHY AND GEOCHEMICAL CHARACTERISTICS

PETROGRAPHY

Andesites in the area of study have porphyritic texture with phenocrysts of dominant plagioclase (20–40% by volume), some clinopyroxene and amphibole (about 2–5% by volume, respectively). All the phenocrysts are euhedral. The groundmass consists mainly of plagioclase (30–70% by volume), together with a few chlorites (about 5% by volume). Dacites in this area are composed of about 20% by volume of euhedral plagioclase phenocrysts and 80% by volume of plagioclase and quartz groundmass. The Nb-enriched basalts also have porphyritic texture with phenocrysts of euhedral plagioclase. The groundmass consists of plagioclase and amphibole. The Fe oxides are abundant in the Nb-enriched basalts. The plagioclase and amphibole were slightly altered, but there was no metamorphism in all the samples.

GEOCHEMICAL CHARACTERISTICS

The geochemical characteristics of the andesitic and dacitic rocks in the study area are very similar to those of the typical adakites that are considered to be derived from the partial melts of subducted oceanic crust (Defant & Drummond 1990; Defant & Kepezhinskas 2001). They have a high Al_2O_3 content (ranging from 15.49 to 18.86%, with an average of 17.55%) (Table 1), and very low heavy rare earth element (HREE) (Yb <1.9 ppm) and Y (<18 ppm) content, together with a high Sr content (>400 ppm) and Sr/Y ratio (>40) (Table 2). Compared to those of andesites, two dacites (FY01, FY12) have similar Al_2O_3, CaO, Na_2O and K_2O content, but apparently a higher SiO_2 content and lower MgO ($Mg^{\#}$) and FeO content. The similar Al_2O_3, CaO and Na_2O content may indicate that the fractional crystallization of plagioclase did not occur, whereas the higher SiO_2 content and lower MgO ($Mg^{\#}$) and FeO content might be caused by the fractional crystallization of pyroxene or

Table 2 Trace element compositions of the samples analyzed by inductively coupled plasma–mass spectrometry (ICP–MS) (ppm)

Sample	Adakites									Nb-enriched basalts							
	A01-2	A03-2	A06-3	A10-2	FY-30	FY-53	FY-63	FY-01	FY-12	A04-1	A05-1	FY-16	FY-20	FY-25	FY-26	FY-52	FY-58	FY-59
Ti	4523	5782	4665	4148	5342	3855	4370	3081	3165	20 188	20 134	9565	12 335	18 093	19 963	12 028	11 750	12 290
V	211	257	200	204	225	99.6	117	78.5	152	196	198	158	215	204	142	169	186	169
Cr	28.8	102	61.9	31.7	45.9	20.9	23.6	17.8	54.7	11.4	11.9	64.2	104	13.7	26.2	55.0	96.3	49.1
Co	22.9	33.5	25.5	17.4	28.6	19.1	21.1	13.4	20.3	21.1	21.8	23.4	34.1	21.2	35.4	24.4	32.7	29.7
Ni	12.3	28.7	22.5	15.3	21.1	24.8	28.6	16.8	27.7	7.99	8.35	12.0	49.8	9.09	30.5	11.6	46.0	24.8
Rb	25.5	18.8	16.3	13.4	14.4	19.5	13.2	25.1	24.8	22.0	26.5	29.8	19.2	10.2	7.57	19.9	12.7	13.2
Sr	1813	1050	503	720	879	923	987	437	1074	695	685	691	618	826	631	675	601	636
Y	15.6	13.8	17.6	18.0	18.4	10.1	10.6	10.6	13.6	63.6	63.6	33.7	39.7	53.9	43.2	36.9	38.9	38.3
Zr	97.1	79.3	94.0	82.1	95.4	113	100	125	87.5	347	342	283	300	335	381	294	274	292
Nb	3.53	3.05	5.15	3.54	3.86	12.4	10.8	11.8	2.70	20.9	20.9	14.2	12.6	19.3	17.7	17.0	16.3	16.9
Ba	784	551	507	688	506	493	377	604	646	634	615	934	606	1139	408	1028	524	602
Hf	2.84	2.37	2.67	2.19	2.59	2.64	2.35	2.91	2.35	7.11	7.10	6.31	6.52	7.44	8.38	7.25	6.78	6.67
Ta	0.24	0.17	0.31	0.20	0.21	0.810	0.627	0.85	0.14	1.09	1.08	0.811	0.869	1.15	1.06	1.19	0.832	0.863
Pb	6.21	4.63	2.79	4.12	6.80	7.15	6.92	9.90	10.5	5.27	7.43	6.89	5.88	8.48	7.96	5.55	6.87	5.78
Th	2.84	1.81	2.86	2.46	2.18	1.94	1.59	3.44	2.60	1.85	1.79	2.10	1.53	1.92	1.48	2.43	1.89	1.54
U	1.32	1.43	1.56	1.25	0.904	0.811	0.644	1.27	1.42	0.727	0.691	0.769	0.691	1.17	1.32	0.770	0.735	0.597
Sr/Y	116	76	29	40	48	91	93	41	79	11	11	21	16	15	15	18	15	17
Nb/U	2.7	2.1	3.3	2.8	4.3	15.3	16.8	9.3	1.9	28.7	30.2	18.5	18.2	16.5	13.4	22.1	22.2	28.3
Ce/Pb	5.2	6.2	13.2	7.1	4.6	4.7	4.4	3.6	2.9	20.1	14.4	10.0	10.5	12.7	7.8	13.9	9.4	10.6
La	15.5	13.8	17.9	14.3	14.6	17.7	15.0	19. 8	15.2	45.8	45.7	31.7	25.8	46.5	31.4	34.9	34.1	34.3
Ce	32.3	28.7	36.9	29.4	31.5	33.4	30.5	35.8	30.0	106	107	69.1	61.4	108	62.4	76.9	64.5	61.3
Pr	4.43	3.98	4.76	3.87	4.31	3.85	3.58	4.00	4.02	15.5	15.4	9.44	8.84	15.4	10.4	10.5	10.7	10.1
Nd	19.1	17.4	20.2	16.8	18.0	13.8	13.4	14.2	15.9	69.1	68.1	39.4	38.7	68.3	42.3	44.0	42.2	40.6
Sm	3.99	3.67	4.28	3.51	4.07	2.54	2.59	2.57	3.28	14.4	14.0	7.96	8.64	13.9	9.40	9.03	8.94	8.48
Eu	1.17	1.06	1.25	1.02	1.25	0.847	0.895	0.76	0.962	4.30	4.19	2.10	2.41	4.11	3.01	2.78	2.48	2.53
Gd	3.68	3.39	4.19	3.57	3.61	2.17	2.30	2.18	2.96	14.2	14.1	7.13	8.36	13.2	8.78	8.49	8.28	7.96
Tb	0.521	0.476	0.592	0.510	0.546	0.329	0.327	0.312	0.425	2.08	2.04	1.16	1.37	2.05	1.40	1.36	1.24	1.19
Dy	2.99	2.68	3.40	2.87	3.38	1.81	1.94	1.87	2.35	11.2	11.0	6.55	7.76	11.1	7.98	7.45	7.57	7.03
Ho	0.587	0.529	0.665	0.590	0.652	0.353	0.387	0.359	0.462	2.14	2.11	1.27	1.49	2.06	1.57	1.44	1.50	1.39
Er	1.58	1.37	1.76	1.73	1.88	1.01	1.05	1.09	1.32	5.76	5.75	3.60	4.22	5.57	4.34	3.97	4.11	3.83
Tm	0.249	0.213	0.277	0.266	0.262	0.137	0.142	0.159	0.179	0.821	0.832	0.539	0.623	0.799	0.620	0.601	0.603	0.544
Yb	1.65	1.37	1.86	1.70	1.77	0.932	0.931	1.04	1.21	5.17	5.14	3.53	4.10	4.92	3.88	3.88	3.68	3.50
Lu	0.274	0.208	0.293	0.273	0.265	0.134	0.133	0.158	0.179	0.812	0.810	0.556	0.650	0.792	0.595	0.617	0.534	0.510

Table 3 Isotopic compositions of the samples

Sample	$^{87}Rb/^{86}Sr$	$^{87}Sr/^{86}Sr$ (2δ)	I_{sr} (t = 375 Ma)	$^{147}Sm/^{144}Nd$	$^{143}Nd/^{144}Nd$ (2δ)	ε_{Nd} (t = 375 Ma)
A03-2	0.051840	0.705177 ± 0.000016	0.70490	0.127561	0.512676 ± 0.000011	+4.06
A06-3	0.093448	0.705154 ± 0.000017	0.70466	0.128005	0.512624 ± 0.000010	+3.02
A10-2	0.053810	0.705079 ± 0.000018	0.70479	0.126503	0.512644 ± 0.000009	+3.48

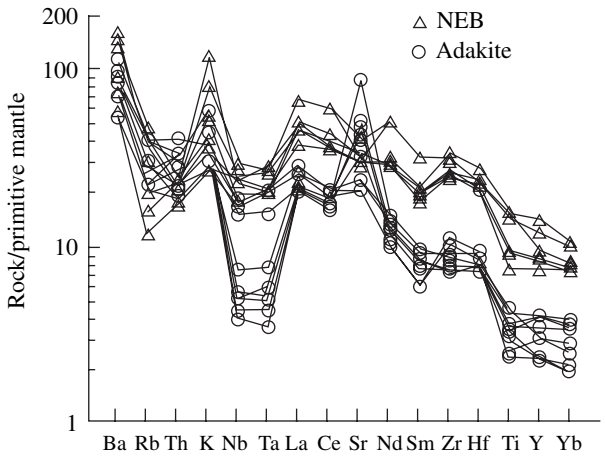

Fig. 2 Primitive mantle-normalized trace element spider diagram of adakites and Nb-enriched basalts (NEB). The primitive mantle normalization value is from Sun and McDonough (1989). See text for discussion.

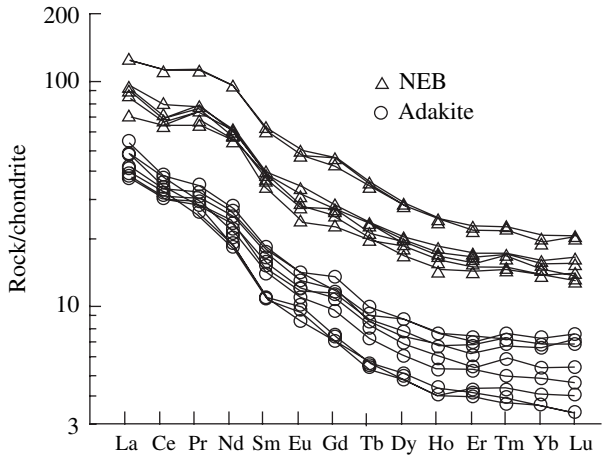

Fig. 3 Chondrite-normalized rare earth element (REE) patterns for adakites and Nb-enriched basalts (NEB). The chondrite normalization value is from Sun and McDonough (1989). See text for discussion.

amphibole. All but three samples show negative Nb and Ta anomalies and a distinct, positive Sr anomaly with very strong high field strength element (HFSE) (Ti, Zr, Hf, Y and Yb) depletion in primitive mantle-normalized trace element patterns (Fig. 2). The chondrite-normalized rare earth element (REE) patterns of andesites and dacites are similar and show apparent HREE depletion and no obvious Eu anomaly (Fig. 3). Since different degrees of partial melting will result in very different REE patterns, it is impossible for the dacites and andesites in this study to be formed by different degrees of partial melting because of their similar REE patterns. At the same time, the petrographic features do not show any evidence of magma mixing. Therefore, the petrography and geochemistry of andesites and dacites show that they might be formed by the fractional crystallization of pyroxene or amphibole.

The basalts are silica-saturated. They are differentiated from normal calc-alkaline arc basalts by their extremely high Nb (between 12.6 and 20.9 ppm), TiO_2 (ranging from 1.85 to 3.66%) and P_2O_5 (more than 0.71%) content and HFSE enrichment with low LILE/HFSE and LREE/HFSE ratios (LILE, large ion lithophile element; LREE, light rare earth element) (Defant *et al.* 1992; Sajona *et al.* 1993; 1994). Compared to those of the primitive mantle, the basalts are enriched in all the trace elements in the spider diagram (Fig. 2). Usually, the circum-Pacific arc Nb-enriched basalts show weakly positive or negative Sr, Ti and Nb anomalies in the primitive mantle-normalized trace element diagram due to their enrichment (Defant *et al.* 1992; Kepezhinskas *et al.* 1996; Sajona *et al.* 1996; 2000; Robles *et al.* 2001). Although the absolute Nb, Sr and Ti content of the basalts in the study area is higher than that of the circum-Pacific Nb-enriched basalts (such as those from the Philippines and Baja, California, and Mexico), the obviously negative Nb, Sr and Ti anomalies appear in the primitive mantle-normalized trace element patterns because of their extremely high REE content (Fig. 2). Their REE content is even higher than that of associated adakites, and it approaches the REE content of bajaiite (Fig. 3). This feature is similar to that of adakites and Nb-enriched basalts from Archean greenstone belts (Hollings & Kerrich 2000; Polat & Kerrich 2001), and also similar to that of the combination of adakite and bajaiite in the Cenozoic era, which strongly suggests that these basalts and andesites are slab melts in origin (Rogers & Saunders 1989).

DISCUSSION

PETROGENESIS OF ADAKITES

Defant and Drummond (1990) suggested that adakites are derived from the partial melting of young and hot subducted slab, whereas Atherton and Petford (1993) argued that the partial melting of newly under-plated basaltic crust at depth should be considered as an alternative way of generating adakites. Yumul *et al.* (2000) considered adakites from the back-arc region of Central Luzon, the Philippines, to be formed by the partial melting of lower crust rather than slab melting. Yogodzinski *et al.* (2001) recently stated that adakites are likely to be formed whenever the margin of a subducting plate is warmed or ablated by a hot mantle flow. Defant and Kepezhinskas (2001) summarized the tectonic processes that can produce adakites, including the partial melting of young and hot subducted slab or remnant slab, oblique or fast subduction, arc–arc collision, initiation of subduction, slab tears and flat subduction. Although studies over the last decade have shown that there are many ways to produce adakites, they can be divided into two general types on the basis of their origin: (i) adakites derived from the partial melting of subducted oceanic slab (Type 1); and (ii) adakites derived from the partial melting of newly under-plated basaltic crust (Type 2).

Although these two types of adakites have some geochemical similarities, distinct geochemical differences (e.g. K_2O and Al_2O_3 content; $Mg^{\#}$ and δSr values) also exist because of their different origins.

In a K_2O versus SiO_2 diagram, Type 1 adakites appear in the tholeiitic to calc-alkaline field, whereas Type 2 adakites mostly appear in the high-K calc-alkaline field (Fig. 4). The K_2O content of adakites from Cordillera Blanca that are thought to be the products of the partial melting of newly under-plated basaltic crust ranges from 2.23 to 3.51%, with the Na_2O/K_2O ratio lying between 1.2 and 2.0 (Atherton & Petford 1993), whereas the Na_2O content of Type 1 adakites is more than 3.5%, with a relatively low K_2O content (Defant & Kepezhinskas 2001). Because the adakites in this study underwent a slight alteration, their alkali earth and fluid mobile element content might have changed, so the K_2O characteristic has been omitted in the discussion of the petrogenesis of adakites in this paper.

Type 2 adakites contain a lower Al_2O_3 content than Type 1 adakites. The Al_2O_3 content of adakites from Cordillera Blanca range from 15.03 to 16.05%, with an average of 15.3%, whereas the average Al_2O_3 content of adakites from circum-Pacific arcs is about 17%. The Al_2O_3 content of the adakites in this study ranges from 15.49 to 18.86%, with an average of 17.55%. It is similar to that of Type 1 adakites.

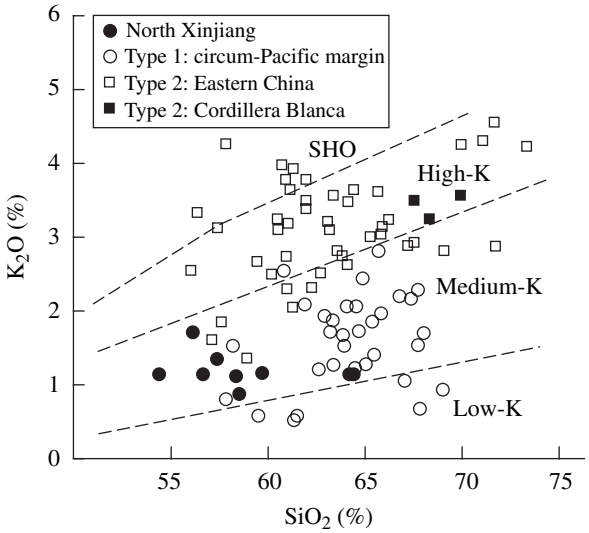

Fig. 4 SiO_2–K_2O diagram. Type 1 adakites and Type 2 adakites are derived from the partial melting of subducted oceanic slab and under-plated basaltic crust, respectively. The data are obtained from Ge *et al.* (2002) for the circum-Pacific Ocean and eastern China; Atherton and Petford (1993) for Cordillera Blanca; and Table 1 for northern Xinjiang.

Experimental results show that the maximum $Mg^{\#}$ value for partial melts of mid-oceanic ridge basalt (MORB) is 45 (Rapp 1997), while typical MORB has an $Mg^{\#}$ value of about 60. The addition of 10% of peridotite can increase the $Mg^{\#}$ value from 44 to 55, and decrease the SiO_2 content (Rapp *et al.* 1999). The average $Mg^{\#}$ value of adakites from the circum-Pacific arcs (Type 1) is about 55, indicating that the ascending adakitic magma interacts with the overlying mantle wedge (Ge *et al.* 2002). It is impossible for Type 2 adakitic magmas to interact with peridotite during their ascent, because there is no overlying mantle wedge. This means that the $Mg^{\#}$ value of Type 2 adakites is always less than 45. For example, the $Mg^{\#}$ value of the adakites from Cordillera Blanca and eastern China ranges from 30 to 45, with an average value of 38 (Atherton & Petford 1993; Ge *et al.* 2002). As for the adakites in this study, the $Mg^{\#}$ value of andesites ranges from 43.8 to 53.5, indicating that the adakitic magmas may have interacted with the overlying mantle wedge peridotite during their ascent. This also leads to lower Sr/Y and La/Yb ratios. The $Mg^{\#}$ value of two dacites are apparently lower (39.3 and 40.7), with

relatively higher SiO_2 content (64.21 and 64.52%), probably because of the fractional crystallization of pyroxene or amphibole.

Defant *et al.* (2002) suggested that adakites contain the typical arc signature: depleted Nb and Ta content and, in most cases, MORB-like Sr and Nd isotope characteristics. The extreme variations in the more incompatible elements, such as Rb, Ba, K etc., may be caused by the sediment incorporated into an adakite during slab melting. It may also affect the isotopic composition of adakites. Bebout *et al.* (1999) found that partial melts of the subducted slab and sediments associated with the hydrous composition in the Catalina schist can also affect the isotopic composition of adakites. The Sr and Nd isotopic compositions of adakites in this study are listed in Table 3. Their $^{87}Sr/^{86}Sr$ and $^{143}Nd/^{144}Nd$ ratios vary from 0.705079 to 0.705177 and 0.512624 to 0.512676, respectively, whereas the SrI and $\varepsilon_{Nd}(t)$ values range from 0.70466 to 0.70490 and 3.02 to 4.06, respectively. The slightly higher SrI and lower $\varepsilon_{Nd}(t)$ values compared to those of MORB (SrI < 0.70365 and $\varepsilon_{Nd}(t) > 5.1$; Pyle *et al.* 1992) indicate that slab sediments were incorporated into the adakites during slab melting in the study area. This also accounts for the relatively lower $Mg^{\#}$ value in the andesites compared to their Cenozoic counterparts.

Therefore, the geochemical characteristics imply that the adakites in this study are linked to the subduction of oceanic slab with slab sediment incorporation, rather than the partial melting of newly under-plated basaltic crust.

PETROGENESIS OF NB-ENRICHED BASALTS

All the Nb-enriched basalts (or high-Nb basalts) that are found worldwide are closely associated with the presence of adakites, whereas adakites can occur alone. This implies that the generation of Nb-enriched basalts is closely related to that of adakites (Defant *et al.* 1992). The Nb-enriched basalts are distinguished from normal arc basalts by their apparently higher Nb, Ti and P_2O_5 content and HFSE enrichment, indicating that their petrogeneses are different from those of normal arc basalts.

Several potential causes of the higher Nb, Ti and P_2O_5 content and HFSE enrichment in the origination of Nb-enriched basalt have been suggested. These are: (i) crustal contamination via either sediment incorporation in the mantle source or assimilation of continental material by ascending magma; (ii) partial melting of the subducted oceanic crust; (iii) partial melting of enriched mantle, such as the source of an oceanic island basalt (OIB); and (iv) presence of a hybridized mantle wedge above the subduction zone (Kepezhinskas *et al.* 1996). Crustal contamination has been rejected as the cause of the higher Nb, Ti and P_2O_5 content and HFSE enrichment in the origination of Nb-enriched basalt because of the extremely enriched LILE that is inconsistent with Nb-enriched basalts, and coexisting calc-alkaline basalts with low HFSE concentrations imply that there is no contamination in many natural cases. Both natural and experimental products of the partial melting of subducted oceanic crust do not resemble Nb-enriched basalts (Sorensen & Grossman 1989; Rapp *et al.* 1991). Although some geochemical features of Nb-enriched basalts are similar to those of OIBs, relatively lower Nb/U and Ce/Pb ratios (47 ± 10 and 25 ± 5 for OIB, respectively; Hofmann *et al.* 1986) in the Nb-enriched basalts eliminate the possibility that they are derived directly from OIB-type mantle (Figs 5,6). Furthermore, the most Nb-enriched basalts have a negative Nb anomaly that is distinctly different from the positive Nb anomalies observed in OIBs, and absolute values of the HFSE in Nb-enriched basalts are frequently lower than those in OIBs. Therefore, many studies show that Nb-enriched basalts might be derived from a slab melt-metasomatized mantle source (Defant *et al.* 1992; Defant & Drummond 1993; Sajona *et al.* 1993; 1996; Kepezhinskas *et al.* 1996).

Both experimental results and case studies in nature in recent years are beginning to suggest

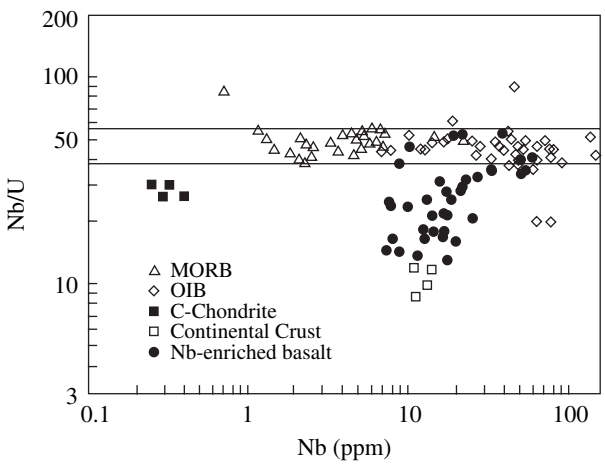

Fig. 5 Nb–Nb/U diagram. The data are obtained from Hofmann *et al.* (1986) for mid-oceanic ridge basalt (MORB), oceanic island basalt (OIB), C-chondrite and continental crust; and Polat and Kerrich (2001), Kepezhinskas *et al.* (1996) and Table 2 for Nb-enriched basalt.

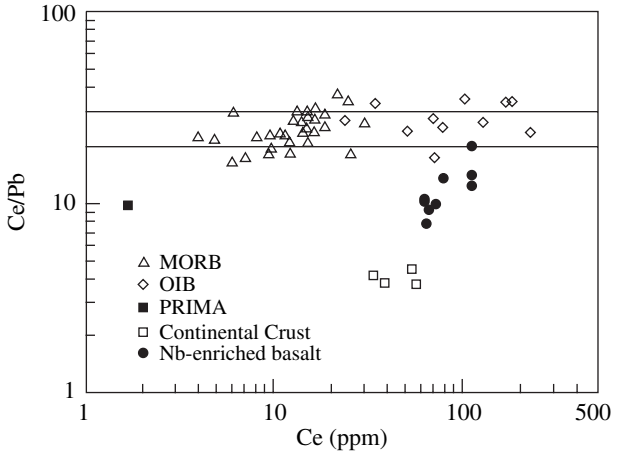

Fig. 6 Ce–Ce/Pb diagram. The data are obtained from Hofmann *et al.* (1986) for mid-oceanic ridge basalt (MORB), oceanic island basalt (OIB), C-chondrite and continental crust; and Table 2 for Nb-enriched basalt.

that slab melts may play an important role in the metasomatism of mantle wedge. Experiments conducted by Sen and Dunn (1994) on the reaction of (adakitic) amphibolite melts with spinel lherzolite show that olivine, clinopyroxene and spinel are consumed and amphibole and Fe-enriched orthopyroxene are precipitated. The experimental results of the reaction between slab-derived melts and peridotite in the mantle wedge also show that olivine is consumed, while Na-amphibole is produced (Rapp *et al.* 1999). The same results are obtained in nature. Schiano *et al.* (1995) found that the melt inclusions in mantle xenoliths from Batan Island, northern Luzon Arc, are similar in composition to adakites. They concluded that slab melts were present during metasomatism of the arc mantle below the Luzon Arc. Quartz diorite veins found in a plagioclase-bearing spinel lherzolite xenolith in alkali basalt from Tallante, Spain, were composed mainly of plagioclase and quartz, with a thin orthopyroxene rim along the olivine wall. This implies that the orthopyroxene rim is formed by the reaction between the melt and olivine (Arai *et al.* 2003). Kelemen *et al.* (1998) pointed out that about 30% of continental upper mantle samples (xenoliths and exposed massifs) are enriched in orthopyroxene (Opx)/olivine relative to the residual peridotite from the partial melting of the primitive mantle. They proposed a two-step process to explain this. First, peridotite with high $Mg^{\#}$ and low Opx is created by a high degree of polybaric melting that stops at pressures lower than 30 kbar. Later, these depleted residues are enriched in Opx by interacting with the SiO_2-rich melts generated mainly by the partial melting of eclogitic basalt and sediment in a subduction zone. Therefore, the interaction between slab-derived melts and mantle wedge peridotite is ubiquitous. Olivine, clinopyroxene and spinel will be consumed, while amphibole and Fe-enriched orthopyroxene will be precipitated during this interaction process.

The interactions between slab melts and mantle wedge peridotite lead to several different results. Yogodzinski *et al.* (1994; 1995) discovered two types of high-Mg andesites in the western Aleutian Komandorsky Island region of Alaska and Russia: Adak and Piip. They suggested that the Adak type is a high-Mg adakite that comes from the limited interaction of adakites with peridotite in the mantle wedge before they are extruded, whereas the Piip type is formed from the direct melting of the mantle wedge after metasomatism by the slab melts. The Setouchi Belt of southwest Japan is also believed to be a Piip-type, high-Mg andesite. Tatsumi and Hanyu (2003) suggested that the possible mechanisms for the production of mantle-derived, high-Mg andesite magams in the Setouchi Belt of southwest Japan, including: (i) partial melting of mantle wedge peridotite by the addition of aqueous fluids from the subducting lithosphere; and (ii) partial melting of the subducting sediments and altered oceanic crust, and subsequent melt–mantle interaction, be examined by the geochemical formulation of dehydration, partial melting and melt-solid reactions. Although both mechanisms can explain the incompatible trace element characteristics of high-Mg andesites, simple hydrous melting of mantle wedge peridotite cannot account for the Sr–Nd–Pb–Hf isotopic compositions of such andesites, whereas the latter mechanism, which is consistent with the thermal structure beneath the Setouchi volcanic belt, can well reproduce the isotopic signature of those high-Mg andesites. Kepezhinskas *et al.* 1996) found HFSE-rich phases along the contact region between the felsic veins and the mantle, and concluded that the reaction preferentially increases the HFSE in the Na-metasomatized mantle. Subsequent melting of this Na-metasomatized mantle produces Nb-enriched basalts or high-Mg andesites. Several studies have suggested that both an adakite and a hydrous slab fluid are involved in the formation of boninites, attesting to the involvement of young crust subduction (Taylor *et al.* 1994). Therefore, Defant *et al.* (2002) proposed the term 'adakite metasomatic volcanic series' for this genetically related volcanic suite of rocks that would incorporate adakite.

As for the minerals in the mantle peridotite that can scavenge for Nb and HFSE during slab melts and mantle peridotite interaction, current data preclude all the common mantle minerals (Cpx, Opx, Ol, Gt and Sp) as the Nb and Ta hosts. The partition coefficients for Nb and Ta are very high for rutile/fluid and rutile/melt pairs, but the low modal abundance of these phases may nevertheless preclude their control of the Nb–Ta signature (Ayers 1998). Although the experimental distribution coefficient (*D*-value) of Nb between amphibole and slab melts is slightly low, ranging from 0.02 to 0.20 (Green 1994), Sajona *et al.* (1993; 1996) stated that amphibole can be expected to be one of the most common Nb-bearing metasomatic phases. Ionov and Hofmann (1995) also suggested that amphibole may be an important phase that controls Nb and Ta in the subarc mantle. Tiepolo *et al.* (2000) pointed out that the partition coefficients between liquids and amphibole for Nb and Ta are strongly dependent on the structure and composition of both amphibole and slab melts. By combining current knowledge of amphibole crystal chemistry and the results of single-crystal structure refinement, they suggested that amphibole may determine the Nb and Ta signature of magmas during mineral/melt fractionation processes in the upper mantle. Hollings and Kerrich (2000) and Polat and Kerrich (2001), however, mentioned amphibole–ilmenite or amphibole–Fe-enriched orthopyroxene as the Nb and Ta hosts. Studies of the trace elements in minerals from metasomatized spinel lherzolite xenoliths in western Victoria, southeastern Australia, show that amphibole and mica increase the concentration of HFSE. The Nb and Zr concentrations in amphibole can reach 160 and 300 ppm, respectively, whereas mica has a Nb content of 58 ppm (O'Reilly *et al.* 1991). Since amphibole is the most common phase during melt–mantle interaction, it must be one of the most common Nb-bearing phases in metasomatized mantle peridotite.

Therefore, Nb-enriched basalts might be derived from the partial melting of the slab melt-metasomatized mantle wedge peridotite.

GENERATION CONDITIONS

Previous studies have indicated that there are some geochemical differences between the Cenozoic and Archean adakites and associated Nb-enriched basalts because of the different conditions under which they are formed. Martin (1999) suggested that the depth of slab melting and the degree of interaction between slab melts and mantle peridotite are closely related to the geothermal gradient. The extremely high geothermal gradient in the Archean era caused the melting of the subducted slab in the relatively shallow plagioclase stability field, whereas the melting of subducted slab in the Cenozoic era could not occur until it descended into the deeper garnet stability field. Experimental studies show that the melts generated at 10 to 40% fusion of the metabasalts or amphibolites are adakitic in composition and equilibrated with residences made up of plagioclase + amphibole ± orthopyroxene ± ilmenite at low pressure (8 kbar), garnet + amphibole ± plagioclase ± clinopyroxene ± ilmenite at 16 kbar and garnet + clinopyroxene ± rutile at higher pressure (Martin 1999). Therefore, higher geothermal gradients (25–30°C/km) and lower pressure (ranging from 8 to 18 kbar) along the Benioff zone in the Archean era could have resulted in relative HREE enrichment in both adakites and Nb-enriched basalts because of the lesser incorporation of garnet in the residue. This also accounts for the absence of a positive Sr anomaly in adakites as a result of some plagioclases remaining in the residual phases. Archean adakites are relatively poorer in transitional elements (e.g. Cr and Ni) and MgO compared to their Cenozoic counterparts, indicating that the mantle–melt interactions were less efficient, probably because of the shallower depth of slab melting. In this case, the slab-derived melts rise through a thinner mantle wedge, thus reducing the efficiency of the interactions (Martin 1999).

The positive Sr anomalies in the adakites in this study indicate that the plagioclase in the source region should almost be melts. So the depth of slab melting in this area should be deeper than that of Archean adakites whose slab melting occurred in the plagioclase stability field. Based on experimental results (Martin 1999), the pressure might be more than 16 kbar (i.e. a slab melting depth of about 55 km) for adakite generation in this area. A slightly higher HREE content of these adakites compared to that of their Cenozoic counterparts implies the lesser incorporation of garnet in the residual phase. It means that the depth of the Paleo-Asian Oceanic slab melting in northern Xinjiang is shallower than the depth of the slab melting in the Cenozoic era, which is about 70–90 km (Martin 1999). Therefore, the depth of the Paleo-Asian Oceanic slab melting lies between the depths of the slab melting in the Archean and Cenozoic eras. The lower transitional element and $Mg^{\#}$ content in the adakites in this study compared to their

Cenozoic counterparts might account for the relatively weak melt–mantle interaction as a result of the slightly shallower slab melting depth. A lower $Mg^{\#}$ content could also be caused by the incorporation of slab sediments during slab melting (Tatsumi & Hanyu 2003). The geochemical features of adakites and Nb-enriched basalts in northern Xinjiang indicate that the geothermal gradient in the Paleo-Asian Oceanic subduction zone and the depth of the Paleo-Asian Oceanic slab melting lie between their counterparts in the Archean and Cenozoic eras.

GEOLOGICAL SIGNIFICANCE

It has been determined that the Paleo-Asian Ocean occurred in northern Xinjiang during the Paleozoic era. High-Mg andesites and Mg-rich dacites of Devonian age in the Ashele area and a back-arc basin ophiolite in Kuerti in the southern margin of the Siberian Plate indicate that the Paleo-Asian Oceanic Plate subducted beneath the Siberian Plate during the late Paleozoic period (Niu *et al.* 1999; Xu *et al.* 2003). As for the timing of the subduction and the closing of the Paleo-Asian Ocean, controversies still exist because of the lack of precise chronological data that can directly indicate the time of the subduction. Some researchers suggested that the orogenesis in the Altay area should have taken place before the late Silurian or early Devonian period (Liu *et al.* 1997; Graupner *et al.* 1999), whereas others believe that the orogenesis between the Siberian Plate and the Kazakhstan-Junggar Plate did not happen until the late Carboniferous–Permian period (Yu *et al.* 1995; Han *et al.* 1997). Jahn *et al.* (2004) suggested that the collage of the Altai Mountains was achieved by strike-slip faulting resulting from two periods of collision: (i) a late Devonian to early Carboniferous oblique subduction and collision of the Gondwana-derived Altai–Mongolian terrane and the Siberian continent; and (ii) a late Carboniferous to Permian closure of the Irtysh-Zaysan branch of the Paleo-Asian Ocean and collision of the Kazakhstan and Siberian continents. Recent studies show that the plagiogranite from the Kuerti back-arc basin ophiolite is derived from the partial melting of amphibolite that is developed from gabbro within the ocean Layer 3 shear zone by low-angle shear deformation during the oceanic crust migrating process. The zircon sensitive high mass-resolution ion microprobe (SHRIMP) U–Pb age of 372 ± 19 Ma for this plagiogranite represents not only the time of the back-arc basin extension and Kuerti ophiolite formation, but also the time of the northward subduction of the Paleo-Asian Oceanic Plate (Zhang *et al.* 2003a).

As for the south side of the Paleo-Asian Ocean, the geological information that is linked to the Paleo-Asian Oceanic Plate subduction is rarely reported. Middle Devonian Boninitic rocks, which may be formed in a forearc setting linked to the southward subduction of the Paleo-Asian Oceanic Plate, have been discovered recently in this region (Fig. 1b) (Zhang *et al.* 2003b). A combination of early Devonian adakite and Nb-enriched basalt that occurred in the northern margin of the Kazakhstan-Junggar Plate and discussed in this paper indicates that the Paleo-Asian Oceanic Plate subducted southward beneath the Kazakhstan-Junggar Plate in the early Devonian era.

CONCLUSIONS

1. The geochemical characteristics of andesitic and dacitic rocks in the northern margin of the Kazakhstan-Junggar Plate show that they are very similar to those of adakites. A relatively high Al_2O_3, Na_2O and MgO content and high $Mg^{\#}$ values indicate that adakites in this area are linked to oceanic slab subduction rather than the partial melting of newly under-plated basaltic crust. They might be derived from the partial melting of the subducted Paleo-Asian Oceanic slab. Slightly higher SrI and lower $\varepsilon_{Nd}(t)$ values than those of MORB imply that slab sediments were incorporated into the adakites during slab melting. Positive Sr anomalies and a slightly higher HREE content in the adakites compared to their Cenozoic counterparts indicate that the geothermal gradient in the Paleo-Asian Oceanic subduction zone and the depth of the Paleo-Asian Oceanic slab melting lie between their counterparts in the Archean and Cenozoic eras.
2. The intercalated basalts are distinguished from the typical arc basalts by their higher Nb and Ti content with HFSE enrichment. They are Nb-enriched basalts and are derived from the partial melting of the slab melt-metasomatized mantle wedge peridotite.
3. The distribution of the adakites and Nb-enriched basalts, together with boninitic rocks in the northern margin of the Kazakhstan-Junggar Plate, indicates that the Paleo-Asian Oceanic slab subducted southward beneath the

Kazakhstan-Junggar Plate in the early Devonian era.

ACKNOWLEDGEMENTS

We are indebted to Professor G. P. Yumul Jr., Dr Carla Dimalanta and Professor Y. G. Xu for their helpful comments on an early version of the manuscript. We sincerely thank the editor, Dr Y. Tamura and two reviewers, Dr J. Kimura and Dr R. Hickey-Vargas for their constructive comments and suggestions. We are also grateful to the Editor-in-Chief, Professor A. Ishiwatari, who made the final corrections to our paper. This work was supported by grants from the National Natural Science Foundation of China (40473016), the Major State Basic Research Program of the People's Republic of China (2001CB409805) and the Chinese Academy of Sciences (GIGCX-03-01 and GIGCX-04-03).

REFERENCES

AMELIN Y. V., NEYMARK L. A., RISTK E. Y. & NEMCHIN A. A. 1996. Enriched Nd-Sr-Pb isotopic signatures in the Dovyren layered intrusion (eastern Siberia, Russia): Evidence for source contamination by ancient upper-crustal material. *Chemical Geology* **129**, 39–69.

AMELIN Y. V., RISTK E. Y. & NEYMARK L. A. 1997. Effects of the interaction between ultramafic tectonite and mafic magma on Nd-Pb-Sr isotopic systems in the Neoproterozoic, Chaya Massif, Baikar-Muya, ophiolite belt. *Earth and Planetary Science Letters* **148**, 299–316.

ARAI S., SHIMIZU Y. & GERVILIA F. 2003. Quartz diorite veins in a peridotite xenolith from Tallante, Spain: Implications for the reaction and survival of slab-derived SiO_2-oversaturated melt in the upper mantle. *Proceedings of the Japan Academy* **79**, pp. 145–50 (Series B).

ATHERTON M. P. & PETFORD N. 1993. Generation of sodium-rich magmas from newly underplated basaltic crust. *Nature* **362**, 144–6.

AYERS J. 1998. Trace element modeling of aqueous fluid–peridotite interaction in the mantle wedge of a subduction zone. *Contributions to Mineralogy and Petrology* **132**, 390–404.

BEBOUT G., RYAN J. G., LEEMAN W. P. & BEBOUT A. E. 1999. Fractionation of trace elements during subduction-zone metamorphism: Effect of convergent margin thermal evolution. *Earth and Planetary Science Letters* **171**, 63–81.

CHEN B. & JAHN B. M. 2004. Genesis of post-collisional granitoids and basement nature of the Junggar Terrane, NW China: Nd–Sr isotope and trace element evidence. *Journal of Asian Earth Sciences* **23**, 691–703.

COLEMAN R. G. 1989. Continental growth of northwest China. *Tectonics* 8, 621–35.

DEFANT M. J. & DRUMMOND M. S. 1990. Derivation of some modern arc magmas by the melting of young subducted lithosphere. *Nature* **347**, 662–5.

DEFANT M. J. & DRUMMOND M. S. 1993. Mount St Helens: Potential example of the partial melting of the subducted lithosphere in a volcanic arc. *Geology* **21**, 547–50.

DEFANT M. J., JACKSON T. E., DRUMMOND M. S. *et al.* 1992. The geochemistry of young volcanism throughout western Panama and southeastern Costa Rica: An overview. *Journal of the Geological Society of London* **149**, 569–79.

DEFANT M. J. & KEPEZHINSKAS P. 2001. Evidence suggests slab melting in arc magmas. *EOS Transactions, American Geophysical Union* **82**, 67–9.

DEFANT M. J., XU J. F., KEPEZHINSKAS P., WANG Q., ZHANG Q. & XIAO L. 2002. Adakites: Some variations on a theme. *Acta Petrologica Sinica* **18**, 129–42.

GE X. Y., LI X. H., CHEN Z. G. & LI. W. P. 2002. Geochemistry and petrogenesis of Jurassic high Sr/low Y granitoids in eastern China: Constraints on crustal thickness. *Chinese Science Bulletin* **47**, 962–8.

GRAUPNER T., KEMPE U., DOMBON E., PATZOLD O., LEEDER O. & SPOONER E. T. C. 1999. Fluid regime and ore formation in the tungsten (-yttrium) deposits of Kyzyltau (Mongolian Altai): Evidence for fluid variability in tungsten–tin ore systems. *Chemical Geology* **154**, 21–58.

GREEN T. H. 1994. Experimental studies of trace-element partitioning applicable to igneous petrogenesis: Sedona, 16 years later. *Chemical Geology* **117**, 1–36.

HAN B. F., WANG S. G., JAHN B. M., HONG D. W., KAGAMI H. & SUN Y. L. 1997. Depleted-mantle source for the Ulungur river A-type granites from north Xinjiang, China: Geochemistry and Nd–Sr isotopic evidence, and implications for Phanerozoic crustal growth. *Chemical Geology* **138**, 135–59.

HE G. Q., HAN B. F., YUE Y. J. & WANG J. H. 1990. Tectonic division and crustal evolution of the Altay Orogenic Belt in China. *Geoscience Xinjiang* **2**, 9–20 (in Chinese, with English abstract).

HOFMANN A. W., JOCHUM K. P., SEUFERT M. & WHITE W. M. 1986. Nb and Pb in oceanic basalts: New constraints on mantle evolution. *Earth and Planetary Science Letters* **79**, 33–45.

HOLLINGS P. 2002. Archean Nb-enriched basalts in the northern Superior Province. *Lithos* **64**, 1–14.

HOLLINGS P. & KERRICH R. 2000. An Archean arc basalt–Nb-enriched basalt–adakite association: The 2.7 Ga Confederation assemblage of the Birch-Uchi greenstone belt, Superior Province. *Contributions to Mineralogy and Petrology* **139**, 208–26.

HU A. Q., JAHN B. M., ZHANG G. X. & ZHANG Q. F. 2000. Crustal evolution and Phanerozoic crustal growth in northern Xinjiang. Nd–Sr isotopic evidence, Part I: Isotopic characterization of basement rocks. *Tectonophysics* **328**, 15–51.

IONOV D. A. & HOFMANN A. W. 1995. Nb–Ta-rich mantle amphiboles and micas: Implications for subduction-related metasomatic trace element fractionations. *Earth and Planetary Science Letters* **131**, 341–56.

JAHN B. M. & CAPDEVILA R. 2000. Continental growth in the Phanerozoic: Evidence from the Central Asian Orogenic Belt. *Episodes* **23**, 133–4.

JAHN B. M., WU F. Y. & CHEN B. 2000. Massive granitoid generation in Central Asia: Nd isotope evidence and implication for continental growth in the Phanerozoic. *Episodes* **23**, 82–92.

JAHN B. M., WINDLEY B., NATAL'IN B. & DOBRETSOV N. 2004. Phanerozoic continental growth in Central Asia. *Journal of Asian Earth Sciences* **23**, 599–603.

KELEMEN P. B., HART S. R. & BERNSTEIN S. 1998. Silica enrichment in the continental upper mantle via melt/rock reaction. *Earth and Planetary Science Letters* **164**, 387–406.

KEPEZHINSKAS P., DEFANT M. J. & DRUMMOND M. S. 1996. Progressive enrichment of island arc mantle by melt–peridotite interaction inferred from Kamchatka xenoliths. *Geochimica Cosmochimica et Acta* **60**, 1217–29.

KEPEZHINSKAS P. K., KEPEZHINSKAS K. B. & PUKHTEL I. S. 1991. Lower Paleozoic oceanic crust in Mongolian caledonides: Sm–Nd isotope and trace element data. *Geophysical Research Letters* **18**, 1301–4.

KHAIN E. V., BIBIKOVA E. V. & KRONER A. 2002. The most ancient ophiolite of the Central Asian foldbelt: U–Pb and Pb–Pb zircon ages for the Dunzhugur complex, Eastern Sayan, Siberia, and geodynamic implications. *Earth and Planetary Science Letters* **199**, 311–25.

KIMURA J.-I., KUNIKIYO K., OSAKA I. *et al.* 2003. Late Cenozoic volcanic activity in the Chugoku area, southwest Japan arc, during back-arc basin opening and reinitiation of subduction. *Island Arc* **12**, 22–45.

KIMURA J.-I., MANTON W. I., SUN C.-H., IIZUMI S., YOSHIDA T. & STERN R. J. 2002. Chemical diversity of the Ueno basalts, central Japan: Identification of mantle and crustal contributions to arc basalts. *Journal of Petrology* **43**, 1923–46.

LI X. H. 1997. Geochemistry of the Longsheng ophiolite from the southern margin of the Yangtze Craton, SE China. *Geochemical Journal* **31**, 323–37.

LIANG X. R., WEI G. J., LI X. H. & LIU Y. 2003. Precise measurement of $^{143}Nd/^{144}Nd$ and Sm/Na ratios using multiple collectors–inductively coupled plasma mass spectrometer (MC–ICPMS). *Geochimica* **32**, 91–6 (in Chinese, with English abstract).

LIU W., LIU C. Q. & MASUDA A. 1997. Complex trace element effects of mixing–fractional crystallization composite processes: Applications to the Alaer granite pluton, Altay Mountains, Xinjiang, northwestern China. *Chemical Geology* **135**, 103–24.

MARTIN H. 1999. Adakitic magmas: Modern analogues of Archean granitoids. *Lithos* **46**, 411–29.

MORRIS P. A. 1995. Slab melting as an explanation of Quaternary volcanism and aseismicity in southwest Japan. *Geology* **23**, 395–8.

NAGAO T., KAKUBUCHI S. & SHIRAKI K. 1997. Quantitative analysis of major and trace elements in rock samples by the fully automated X-ray spectrometer Rigaku/RIX 3000. *Report of the Center for Instrumental Analysis, Yamaguchi University* **5**, 10–15 (in Japanese).

NIU H. C., XU J. F., YU X. Y., CHEN F. R. & ZHENG Z. P. 1999. Discovery of Mg-rich volcanic rock series in the western Altay area, Xinjiang, and its geologic significance. *Chinese Science Bulletin* **44**, 1685–7.

O'REILLY S. Y., GRIFFIN W. L. & RYAN C. G. 1991. Residence of trace elements in metasomatized spinel lherzolite xenoliths: A proton-microprobe study. *Contributions to Mineralogy and Petrology* **109**, 98–113.

POLAT A. & KERRICH R. 2001. Magnesian andesites, Nb-enriched basalt-andesites, and adakites from late-Archean 2.7 Ga Wawa greenstone belts, Superior Province, Canada: Implications for late Archean subduction zone petrogenetic processes. *Contributions to Mineralogy and Petrology* **141**, 36–52.

PYLE D. G., CHRISTIE D. M. & MAHONEY J. J. 1992. Resolving an isotopic boundary within the Australian-Antarctic Discordance. *Earth and Planetary Science Letters* **112**, 161–78.

RAMSEY M. H., POTTS P. J., WEBB P. C., WATKINS P., WATSON J. S. & COLES B. J. 1995. An objective assessment of analytical method precision: Comparison of ICP–AES and XRF for the analysis of silicate rocks. *Chemical Geology* **124**, 1–19.

RAPP R. P. 1997. Heterogeneous source regions for Archean granitoids. *In* WIT DE M. J. & ASHWAL L. D. (eds). *Greenstone Belts*. Oxford University Press, Oxford.

RAPP R. P., SHIMIZU N., NORMAN M. D. & APPLEPATE G. S. 1999. Reaction between slab-derived melts and peridotite in the mantle wedge: Experimental constraints at 3.8 GPa. *Chemical Geology* **160**, 335–56.

RAPP R. P., WATSON E. B. & MILLER C. F. 1991. Partial melting of amphibolite/eclogite and the origin of Archaean trondhjemites and tonalities. *Precambrian Research* **51**, 1–25.

ROBLES A. A., CAIMUS T., BENOIT M. *et al.* 2001. Late Miocene adakites and Nb-enriched basalts from Vizcaino Peninsula, Mexico: Indicators of East Pacific Rise subduction below southern Baja California? *Geology* **29**, 531–4.

ROGERS G. & SAUNDERS A. D. 1989. Magnesian andesites from Mexico, Chile and the Aleutian Islands: Implications for magmatism associated with ridge-

trench collision. *In* CRAWFORD A. J. (ed.). *Boninites*, pp. 417–45. Unwin-Hyman, London.

SAJONA F. G., BELLON H., MAURY R. C., PUBELLIER M., COTTEN J. & RANGIN C. 1994. Magmatic response to abrupt changes in geodynamic settings: Pliocene-Quaternary calc-alkaline lavas and Nb-enriched basalts of Leyte and Mindanao (Philippines). *Tectonophysics* **237**, 47–72.

SAJONA F. G., MAURY R. C., BELLON H., COTTEN J. & DEFANT M. J. 1993. Initiation of subduction and the generation of slab melts in western and eastern Mindanao, Philippines. *Geology* **21**, 1007–10.

SAJONA F. G., MAURY R. C., BELLON H., COTTEN J. & DEFANT M. J. 1996. High field strength element enrichment of Pliocene-Pleistocene island arc basalts, Zamboanga Peninsula, western Mindanao (Philippines). *Journal of Petrology* **37**, 693–726.

SAJONA F. G., MAURY R. C., PUBELLIER M., LETERRIER J., BELLON H. & COTTEN J. 2000. Magmatic source enrichment by slab-derived melts in a young post-collisional setting, central Mindanao (Philippines). *Lithos* **54**, 173–2006.

SCHIANO P., CLOCCIATTI R., SHIMIZU N. *et al.* 1995. Hydrous, silica-rich melts in the sub-arc mantle and their relationship with erupted lavas. *Nature* **377**, 595–600.

SEN C. & DUNN T. 1994. Dehydration melting of a basaltic composition amphibolite at 1.5 GPa and 2.0 GPa: Implication for the origin of adakites. *Contributions to Mineralogy and Petrology* **117**, 394–409.

SENGÖR A. M. C., NATAL'IN B. A. & BURTMAN V. S. 1993. Evolution of the Altaid tectonic collage and Phanerozoic crustal growth in Eurasia. *Nature* **364**, 299–307.

SORENSEN S. S. & GROSSMAN J. N. 1989. Enrichment of trace elements in garnet amphibolites from the paleo-subduction zone: Catalina Schist, southern California. *Geochimica Cosmochimica et Acta* **53**, 3155–77.

SUN S. S. & MCDONOUGH W. F. 1989. Chemical and isotopic systematics of oceanic basalts: Implications for mantle composition and processes. *In* SAUNDERS A. D. & NORRY M. J. (eds). *Magmatism in the Ocean Basins*, Geological Society Special Publication 42, pp. 313–45. Geological Society of London and Blackwell Scientific Publications, London.

TAMURA Y., YUHARA M., ISHII T., IRINO N. & SHUKUNO H. 2003. Andesites and dacites from Daisen Volcano, Japan: Partial to total remelting of an andesite magma body. *Journal of Petrology* **44**, 2243–60.

TATSUMI Y. & HANYU T. 2003. Geochemical modeling of dehydration and partial melting of subducting lithosphere: Toward a comprehensive understanding of high-Mg andesite formation in the Setouchi volcanic belt, SW Japan. *Geochemistry Geophysics Geosystems* **4**, DOI: 10.1029/2003GC000530.

TAYLOR R. N., NESBITT R. W., VIDAL P., HARMON R. S., AUVRAY B. & CROUDACE I. W. 1994. Mineralogy, chemistry, and genesis of the boninite series volcanics, Chichijima, Bonin Islands, Japan. *Journal of Petrology* **35**, 577–617.

TIEPOLO M., VANNUCCI R., OBERTI R., FOLEY S., BOTTAZZI P. & ZANETTI A. 2000. Nb and Ta incorporation and fractionation in titanian pargasite and kaersutite: Crystal–chemical constraints and implications for natural systems. *Earth and Planetary Science Letters* **176**, 185–201.

XIAO X. C., TANG Y. Q., FENG Y. M., ZHU B. Q., LI J. Y. & ZHAO M. 1992. *Tectonic Evolution of the Northern Xinjiang and its Adjacent Region.* Geological Publishing House, Beijing (in Chinese, with English abstract).

XU J. F., PATERNO R. C., CHEN F. R., NIU H. C., YU X. Y. & ZHENG Z. P. 2003. Geochemistry of late Paleozoic mafic igneous rocks from the Kuerti area, Xinjiang, northwest China: Implications for back-arc mantle evolution. *Chemical Geology* **193**, 137–54.

YOGODZINSKI G. M., KAY R. W., VOLYNETS O. N., KOLOSKOV A. V. & KAY S. M. 1995. Magnesian andesite in the western Aleutian Komandorsky region: Implication for slab melting and processes in the mantle wedge. *Geological Society of America. Bulletin* **107**, 505–19.

YOGODZINSKI G. M., LEES J. M., CHURIKOVA T. G., DORENDORF F., WOERNER G. & VOLYNETS O. N. 2001. Geochemical evidence for the melting of subducting oceanic lithosphere at plate edges. *Nature* **409**, 500–4.

YOGODZINSKI G. M., VOLYNETS O. N., KOLOSKOV A. V., SELIVERSTOV N. I. & MATUENKOV V. V. 1994. Magnesian andesites and the subduction component in a strongly calc-alkaline series at Piip Volcano, far western Aleutians. *Journal of Petrology* **35**, 163–204.

YU X. Y., MEI H. J. & JIANG F. Z. 1995. *Ereqisi Volcanic Rocks and their Mineralization.* Science Publishing House, Beijing (in Chinese).

YUMUL G. P., DIMALANTA C. B., BELLON H. *et al.* 2000. Adakitic lavas in the Central Luzon back-arc region, Philippines: Lower crust partial melting products? *Island Arc* **9**, 499–512.

ZHANG H. X., NIU H. C., TERADA K., YU X. Y., SATO H. & ITO J. 2003a. SHRIMP U–Pb dating of plagiogranite from Kuerti Ophiolite, Altay, Northern Xinjiang. *Chinese Science Bulletin* **48**, 2231–5.

ZHANG H. X., NIU H. C., YU X. Y., SATO H., ITO J. & SHAN Q. 2003b. Geochemical characteristics of Shaerbulake boninites and their tectonic significance, Fuyun County, northern Xinjiang, China. *Geochimica* **32**, 155–60 (in Chinese, with English abstract).